Electronic Supplementary Information (ESI) to:

EXAFS and FTIR studies of selenite and selenate sorption by alkoxide-free sol-gel generated Mg-Al-CO_3 layered double hydroxide with very labile interlayer anions

DOI: 10.1039/c4ta03463e

Natalia Chubar[12*]

[1*]School of Engineering and Built Environment, Glasgow Caledonian University, Cowcaddens Road 70, G40BA, Glasgow, Scotland, United Kingdom

[2]Department of Earth Sciences, Faculty of Geosciences, Utrecht University, Budapestlaan 4, 3584CD, Utrecht, The Netherlands

* Natalia Chubar, Natalia.Chubar@gcu.ac.uk

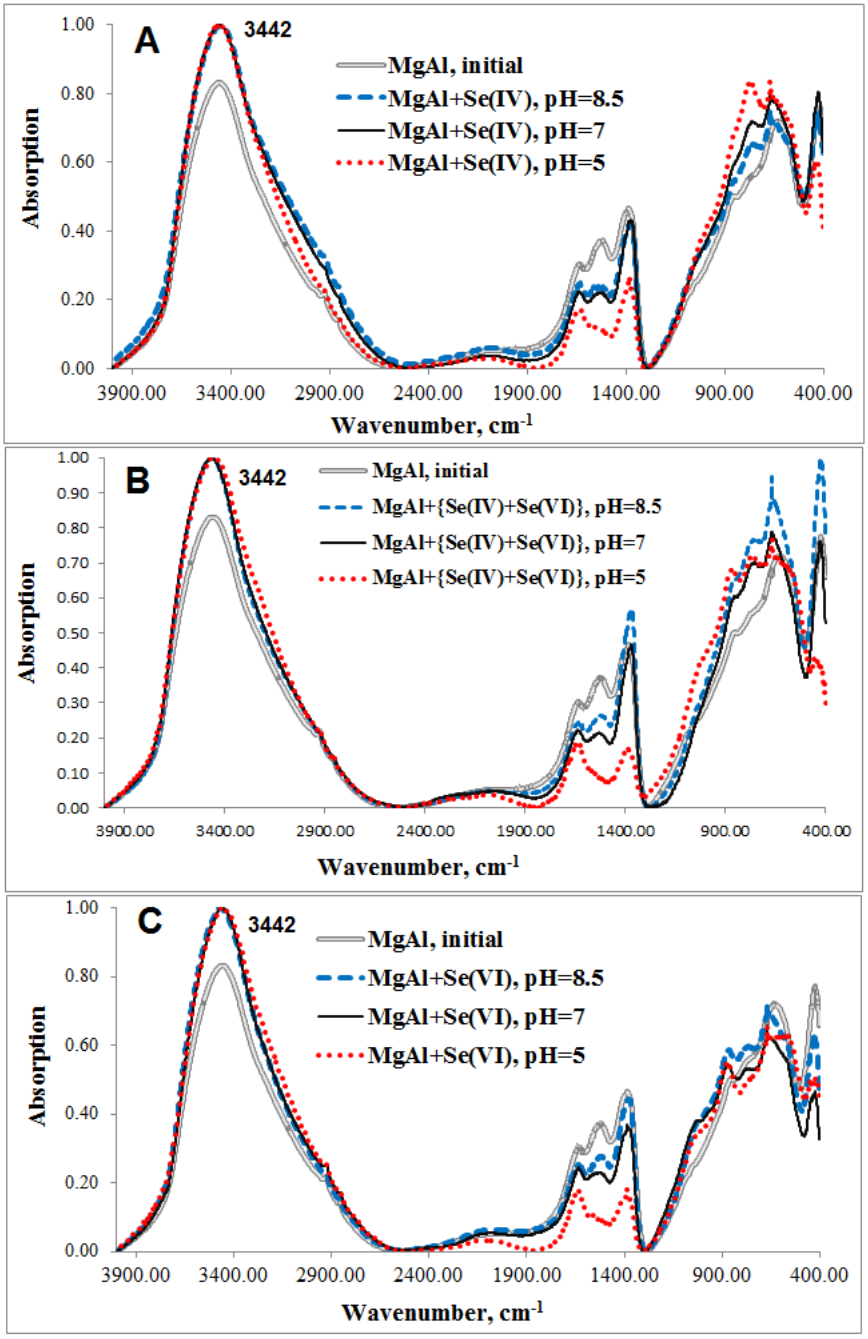

Fig. S1. FTIR spectra of Mg-Al LDH contacted to selenite (A), two selenium water species (selenite+selenate) (B) and selenate (C) at pH 5, 7 and 8.5. More details on the region 400-2000 cm^{-1} are shown in the main body of the paper and in the Fig. 1.

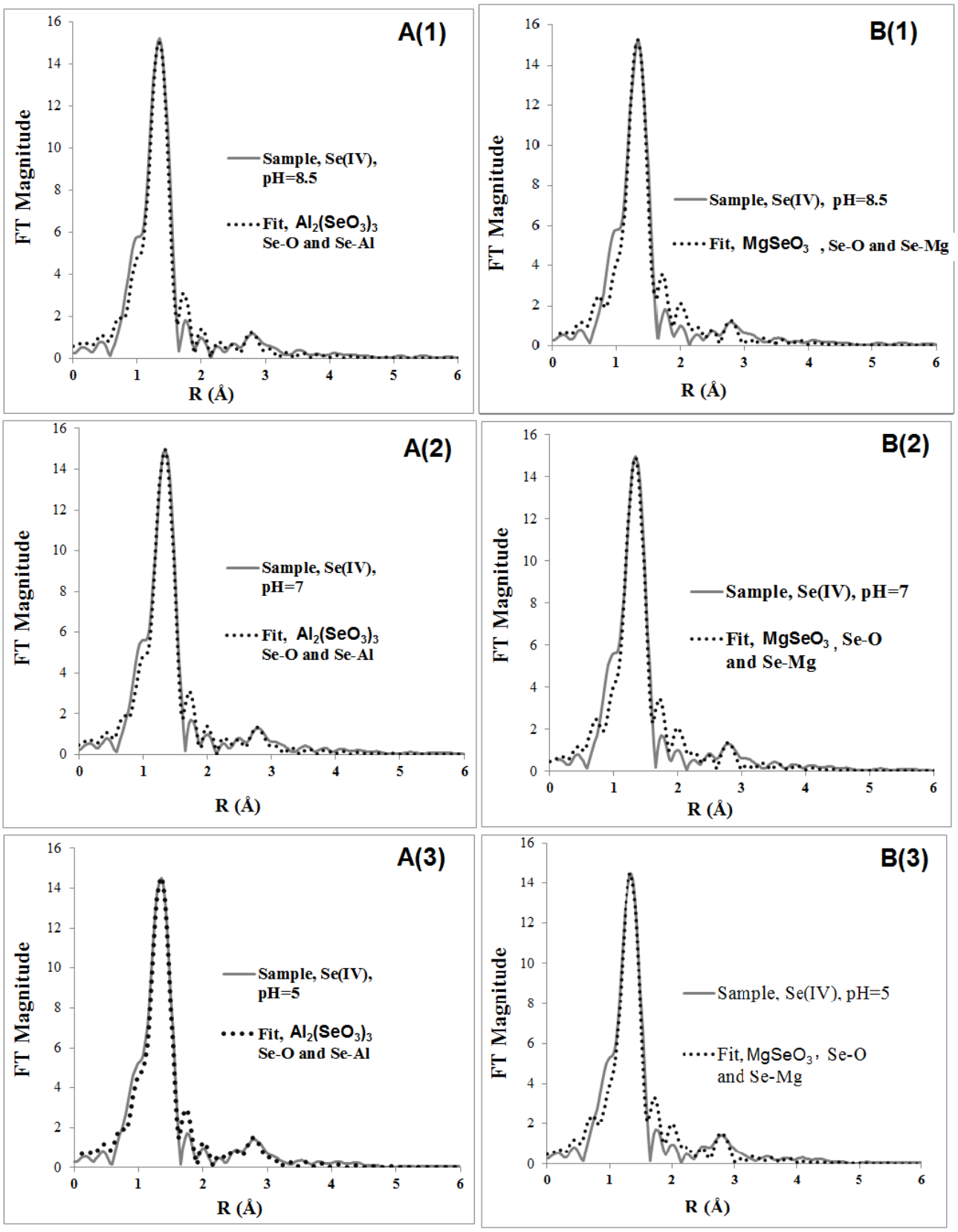

Fig. S2. Fit results (by Artemis) of Se K-edge EXAFS of Se-contained Mg-Al LDHs resulted from selenite sorption by these materials at pH 8.5 (1), 7 (2) and 5 (3). Feff inp files were generated using the atomic coordinates of aluminium (A) and magnesium (B) selenites calculated by Harrison [1] and Johnston [2]. Calculations resulted from these fits are shown in Table 1 (the paper). Two paths calculated by Feff were used for the fitting: Se-O (the first 100%) and Se-Al (in case of aluminium selenite), or Se-O and Se-Mg (in case of magnesium selenite).

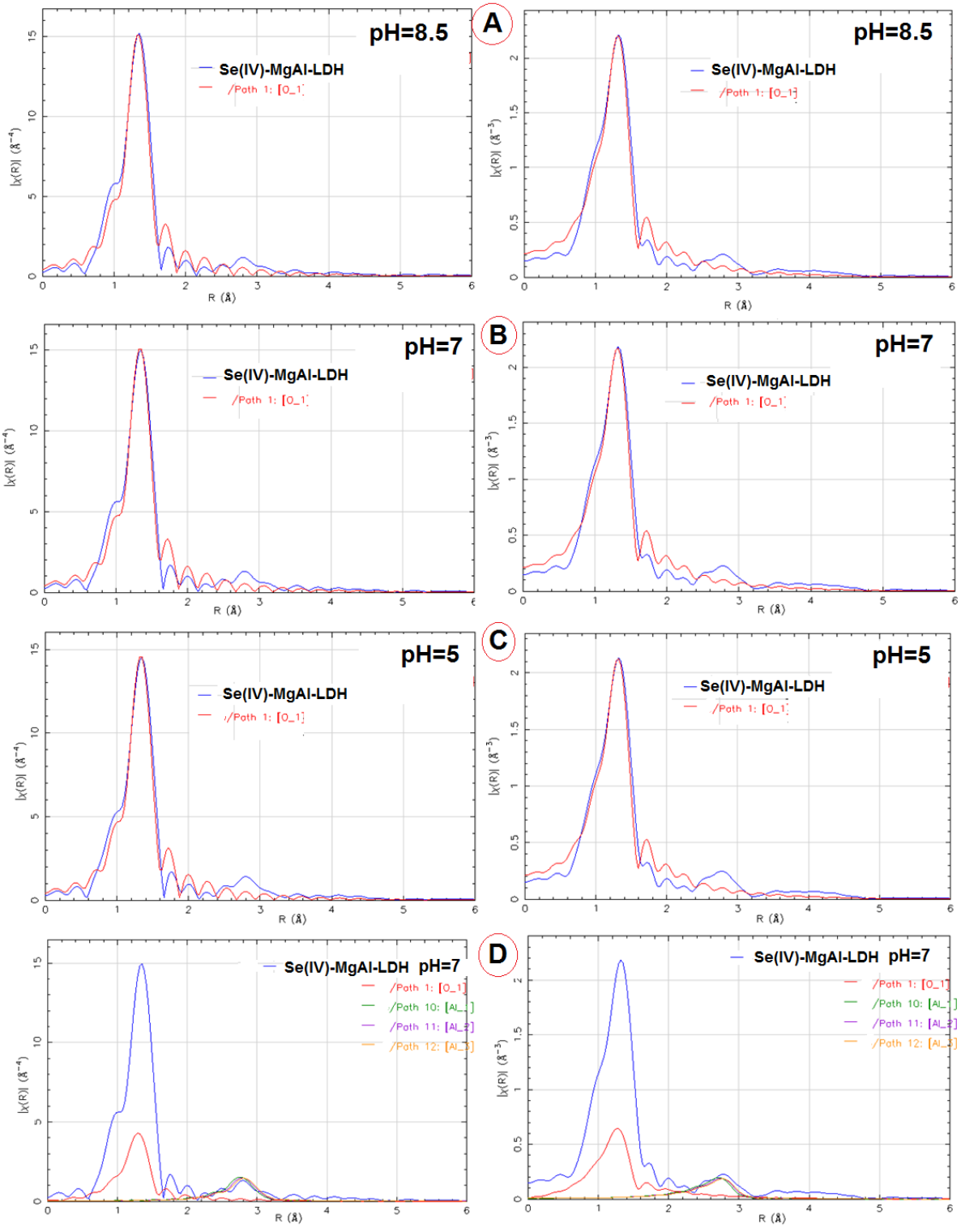

Fig. S3. Artemis fits of Se K-edge EXAFS of Se-sorbed Mg-Al LDHs equilibrated to selenite at pH 8.5 (A), 7 (B) and 5(C) using Feff.inp generated from $Al_2(SeO_3)_3$ [1]. The fitting was done using only one path, Se-O. Se-O and Se-Al paths are plotted together with the experimental Se K-edge EXAFS at pH=7 (D). Fitting was done using k^3 and k^2 weighted EXAFS data shown correspondingly on the left and on the right.

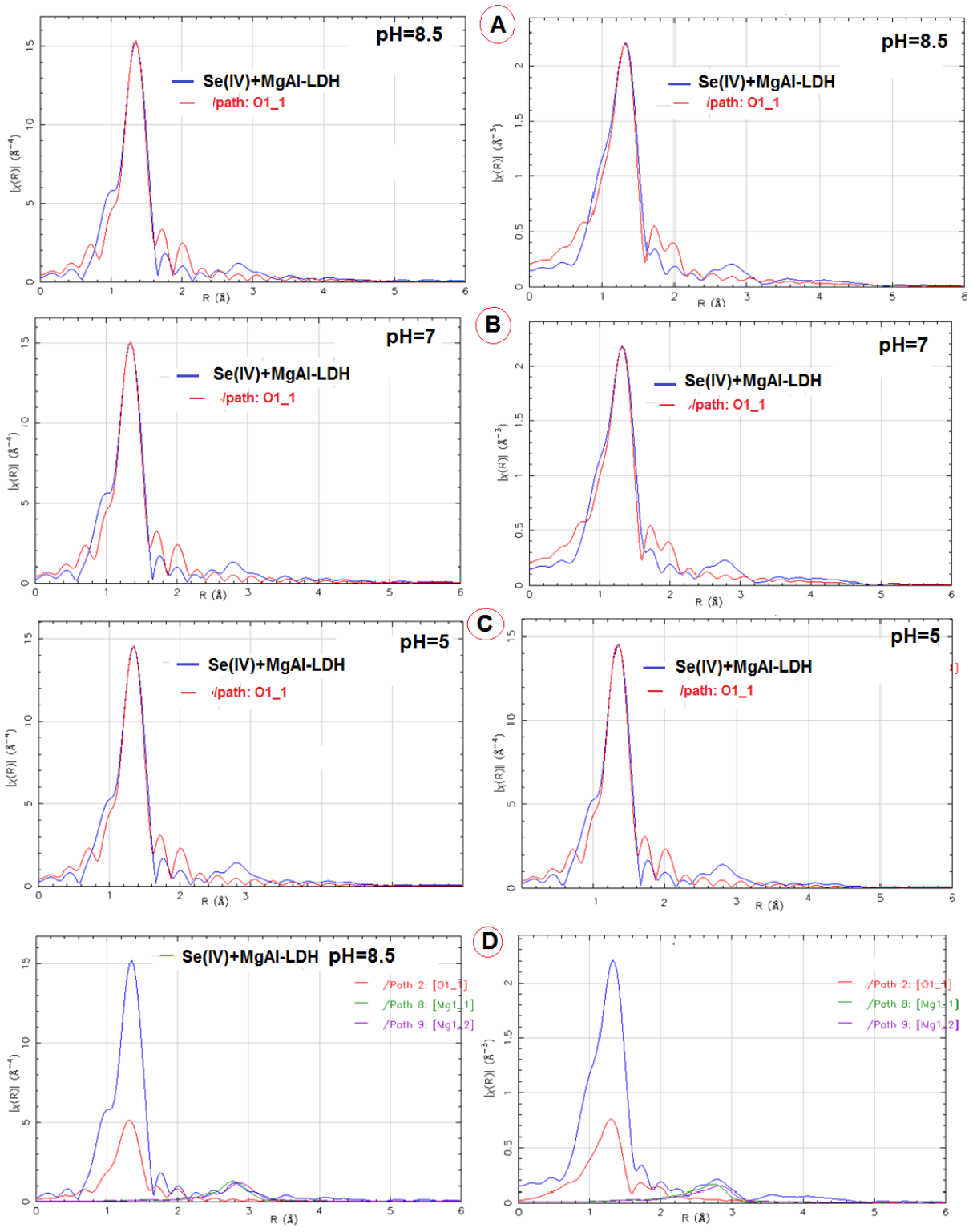

Fig. S4. Artemis fits of Se K-edge EXAFS of Se-sorbed Mg-Al LDHs equilibrated to selenite at pH 8.5 (A), 7 (B) and 5(C) using Feff.inp from $MgSeO_3$ [2]. Only one path, Se-O, was used for fitting. Se-O and Se-Mg paths are plotted together with the experimental Se K-edge EXAFS at pH=7 (D). k^3 and k^2 weighted EXAFS data were used for the fitting shown on the left and on the right correspondingly

To distinguish O from Al/Mg backscattering due to Se oscillations in the second shell, fitting to only the Se-O path was also performed. Figure S3 shows the fits to the first Se-O path for Se(IV)-containing Mg-Al LDHs at pH 8.5, 7 and 5 (Figs. S3A, S3B and S3C, respectively). The relevant paths were plotted together with the Fourier Transforms of the experimental samples. Path 1 (Se-O_1, amplitude=100, R effective = 1.679), path 10 (Se-Al_1, amplitude=22.3 and R effective = 3.18), path 11 (Se-Al_2, amplitude=21.6 and R effective = 3.21) and path 12 (Se-Al_3, amplitude=21.2 and R effective = 3.23) are plotted in Fig. S3D. Note that the raw Feff data were used and that the coordination number in the first shell was not changed (it was left as CN=1), which resulted in a low peak for the Se-O path. Both k^3-(on the left) and k^2- (on the right) weighted Fourier transforms of the Se-K-edge EXAFS were used for the fitting.

Fig. S4 shows the fits based on the atomic coordinates of theoretical $MgSeO_3$ at pH 8.5, 7 and 5 (Figure S4A, S4B and S4C, respectively). The relevant paths are plotted together with the Fourier Transforms of the experimental samples in Figure S4D: path 2 (Se-O_1, amplitude=63.3, R effective = 1.7), path 8 (Se-Mg_1, amplitude=13.3 and R effective = 3.21), path 9 (Se-Mg_2, amplitude=13.6 and R effective = 3.31) and path 10 (Se-Mg_3, amplitude=12.5 and R effective = 3.32). Note that raw Feff data were used and that the coordination number in the first shell was not changed (it was left as CN=1), which resulted in a low peak for the Se-O path compared to the experimental spectrum. Both k-3 (on the left) and k-2 (on the right) weighted χ data were used for the fitting.

To support the conclusion that the smaller peak of the doublet at ~2.6-2.8 Å resulted from Se-O oscillations, the nearest Se-O paths at the same distance with reasonably high amplitude were plotted together with the Se-Al and Se-Mg paths (Fig. S5).

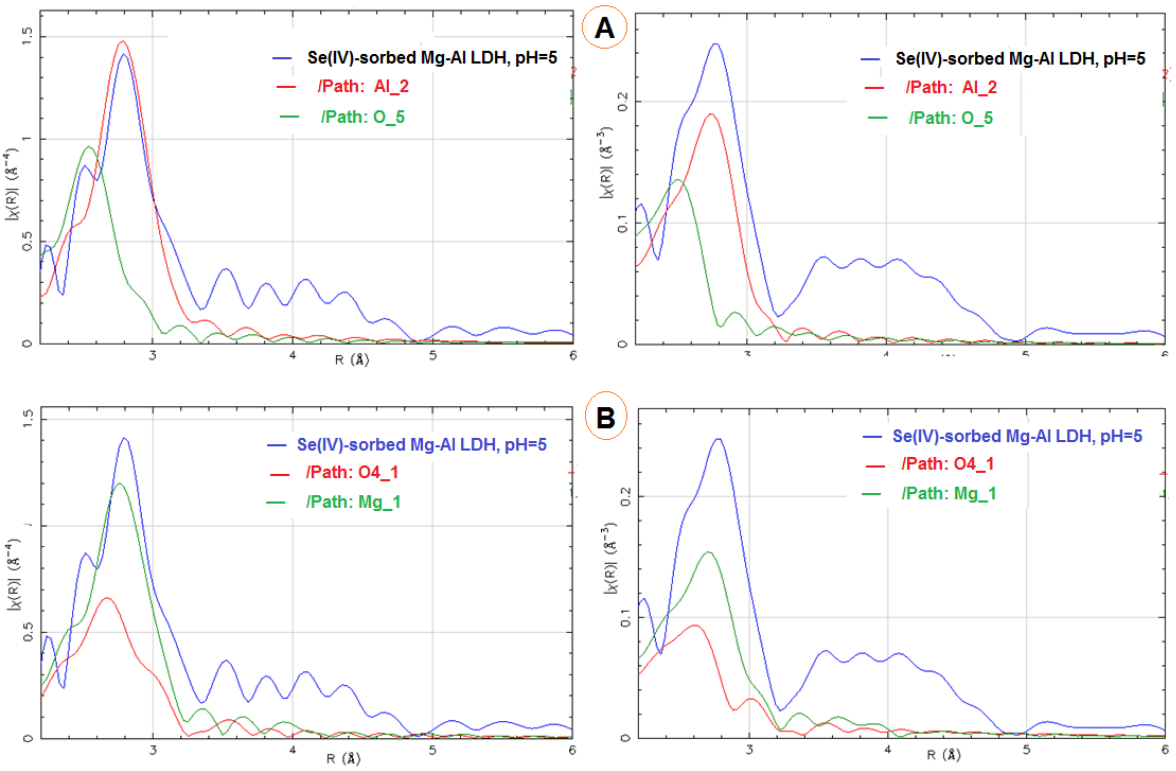

Fig. S5. The nearest Se-O and Se-Al/Mg oscillations in the second shells calculated by Feff using atomic coordinates of $Al_2(SeO_3)_3$ (A) [1] and $MgSeO_3$ (B) [2]. k^3 and k^2 weighted EXAFS data are shown on the left and on the right correspondingly.

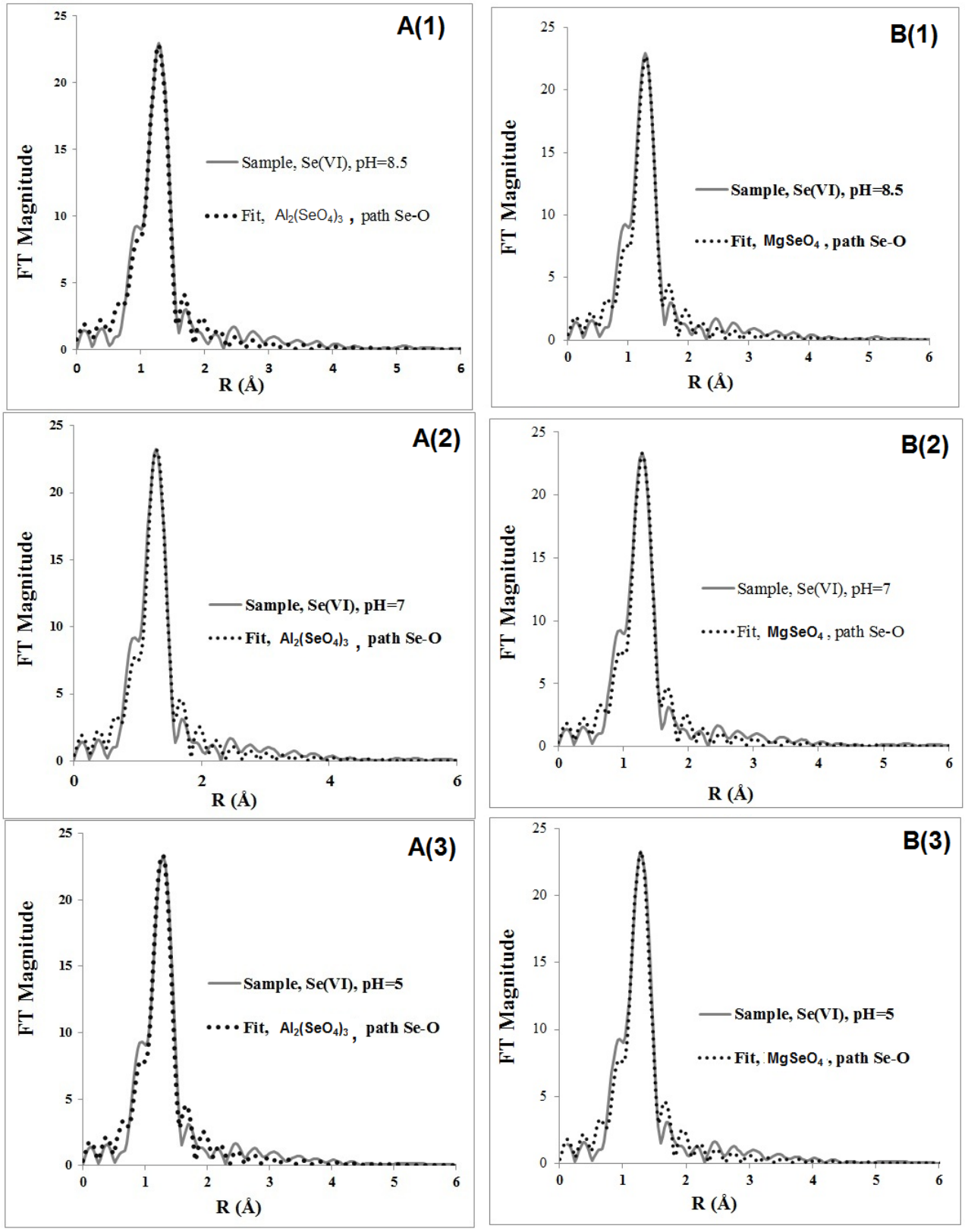

Fig. S6. Fit results (by Artemis) of Se K-edge EXAFS of Se(VI)-sorbed Mg-Al LDHs at pH 8.5 (1), 7 (2) and 5 (3) using Se-O path. Feff.inp files were generated using the atomic coordinates of aluminium (A) and magnesium (B) selenates calculated (correspondingly) by Krivovichev [3] and Kolitsch [4]. Calculations from these fits are shown in Table 2 (the main body of the work).

Fig. S7 shows the paths generated by Feff using the atomic coordinates of highly hydrated aluminum selenate ($[Al(H_2O)_6]_2(SeO_4)_3(H_2O)_4$) [3] (A), anhydrous aluminum selenate [5] (B) and magnesium selenate hexahydrate, $MgSeO_4 \bullet 6H_2O$ [4] (C). These data were prepared to understand the possible contributions from the inner sphere complexation to the binding of selenate by the highly hydrated aluminium--magnesium layered double hydroxides.

Fig. S7 shows that, for the highly hydrated references, Feff did not find oscillations from Se to Mg and Al at a distance that would be sufficiently short for chemisorption interactions. The nearest two Se-Al paths generated for the hydrated aluminum selenate [4] have effective R values of 4.657 and 4.667 Å with a low amplitude of 7 (Figure S7A).

The nearest Se-Mg path generated from the theoretical hydrated magnesium selenate [4] has an effective R value of 4.61 with an amplitude of 7.52 (Figure S7C).

Feff generated using Se-Al paths from the theoretical anhydrous aluminum selenate [5] had effective R values from 3.25 to 3.38 Å. At such distances between the atoms, inner-sphere complexation can take place, but the first Se-O path for the same theoretical reference has an effective R value of 1.47 Å, which is too short for good fits of the first coordination shell of the experimental spectra of the investigated Mg-Al LDH with sorbed selenate. This result means that the anhydrous reference is not suitable for fitting the experimental data from selenate sorption by the highly hydrated Mg-Al LDHs.

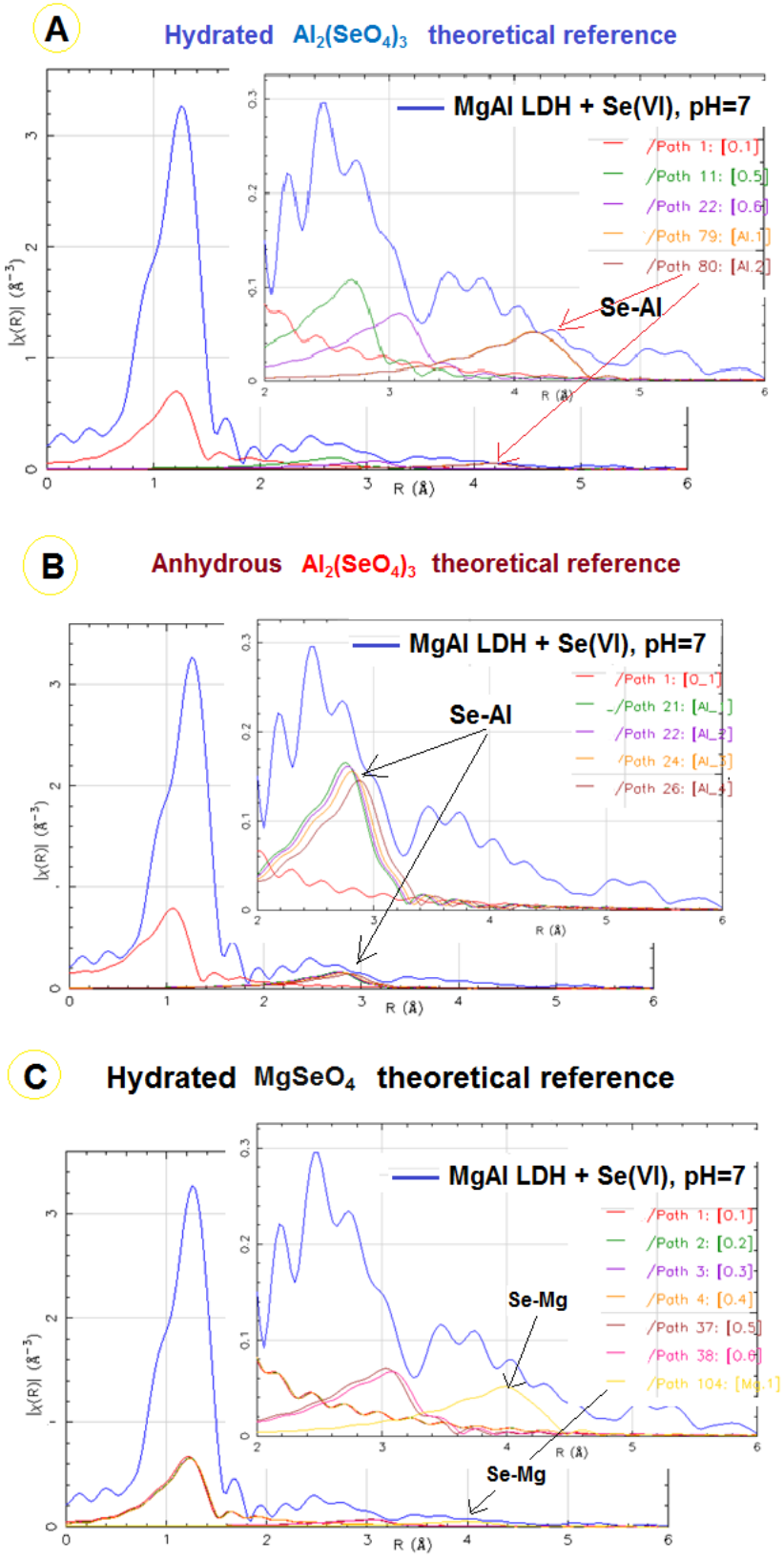

Fig. S7. Paths generated by Feff using the atomic coordinates of the highly hydrated aluminium selenate ($[Al(H_2O)_6]_2(SeO_4)_3(H_2O)_4$) [3] (A), anhydrous aluminium selenate [5] (B) and magnesium selenate hexahydrate, $MgSeO_4 \cdot 6H_2O$ [4] (C).

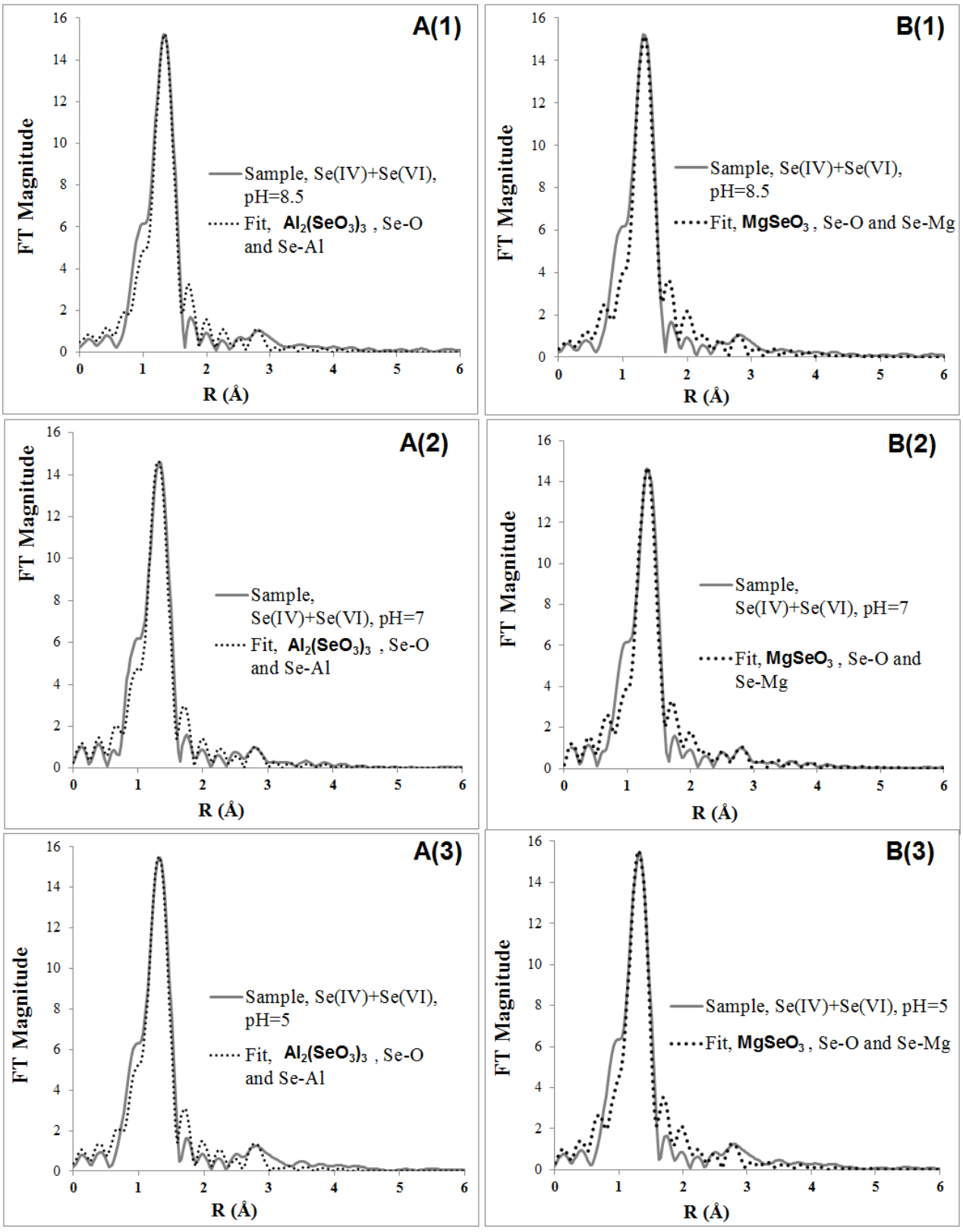

Fig. S8. Fit results (by Artemis) of Se K-edge EXAFS of {Se(IV)+Se(VI)}-contained Mg-Al LDHs resulted from selenium aqueous species sorption at pH 8.5 (1), 7 (2) and 5(3). Feff inp files were generated using the atomic coordinates of aluminium (A) and magnesium (B) selenites calculated by Harrison [1] and Johnston [2]. Two paths calculated by Feff were used for the fitting: Se-O (the first 100%); and Se-Al (in case of aluminium selenite), or Se-O and Se-Mg (in case of magnesium selenite). Calculations from these fits are shown in Table 3 (the paper).

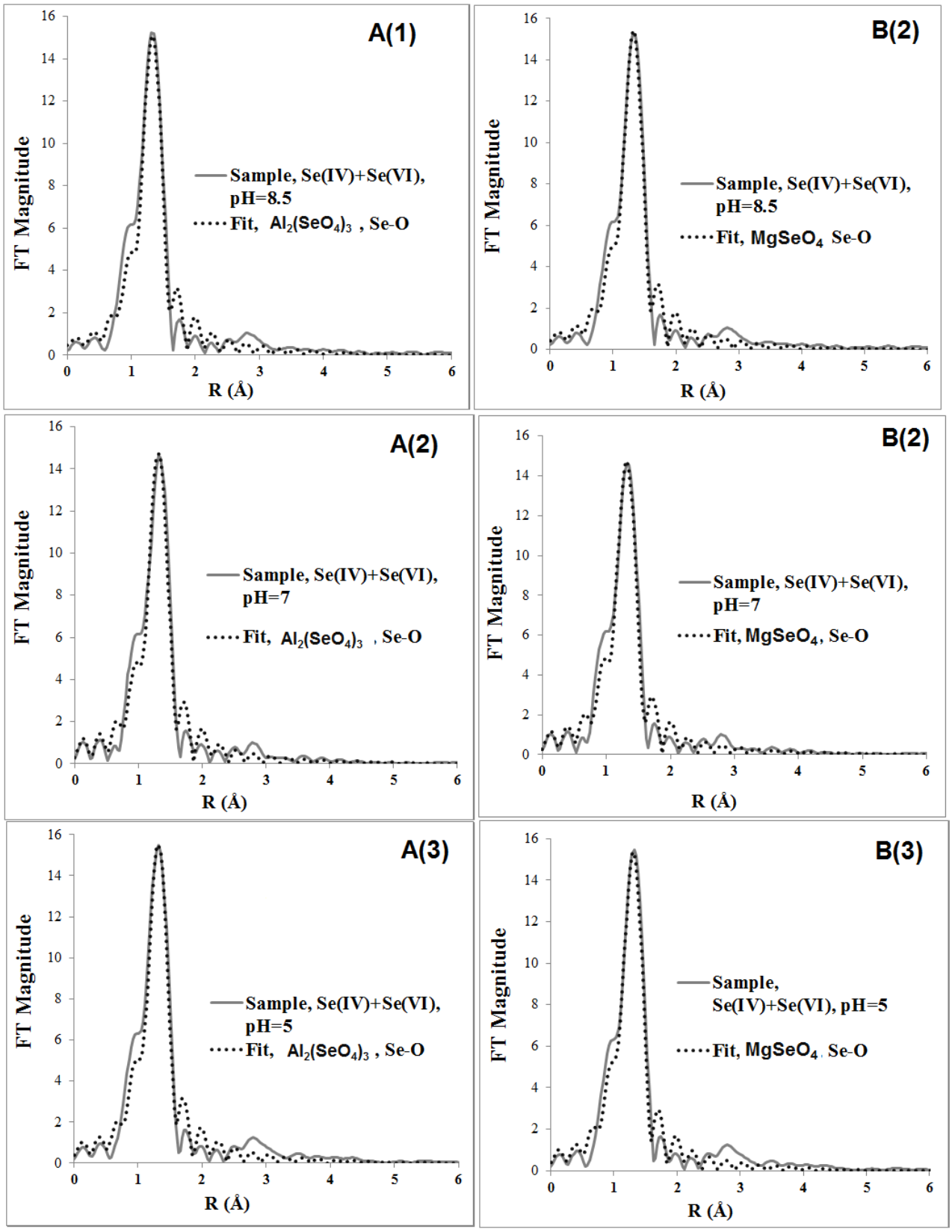

Fig. S9. Fit results (by Artemis program) of Se K-edge EXAFS of Se-contained Mg-Al LDHs resulted from sorption of {selenite+selenite} at pH 8.5 (1), 7 (2) and 5 (3). Feff inp files were generated using the atomic coordinates of aluminium (A) and magnesium (B) selenates calculated by Krivovichev [3] and Kolitsch [4]. Only one path, Se-O, was used for the fitting. Calculations from these fits are shown in Table 3 (the main body of the work).

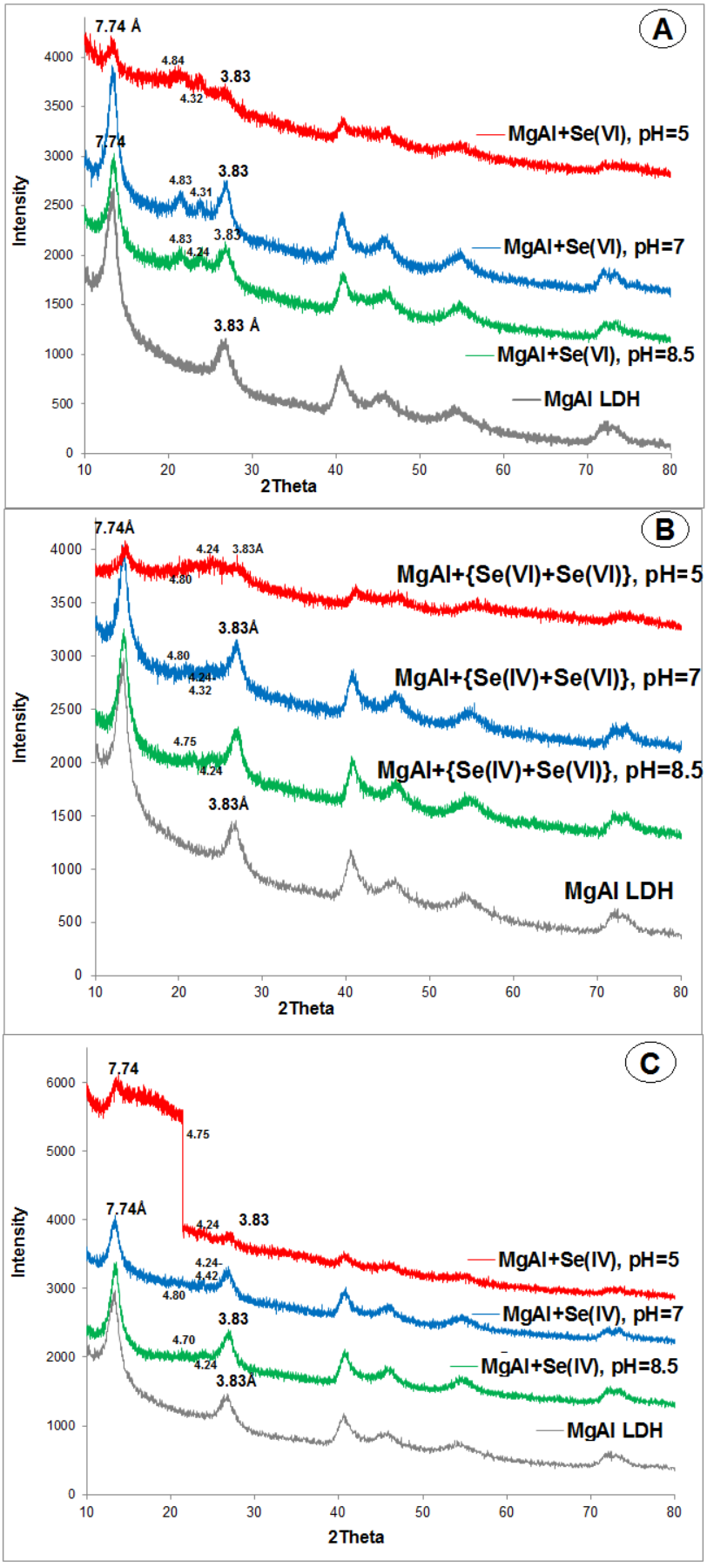

Fig. S10. XRD patterns of the initial MgAl-CO_3 LDHs and with sorbed selenate (A), {selenate+selenite} (B) and selenite (C) at pH 5, 7 and 8.5.

Fig. S10 shows XRD patterns of Mg-Al LDHs with sorbed selenate (A), {selenite+selenate} (B) and selenite (C) in comparison with XRD of the initial material. XRD patterns were in agreement with the rest of the data of this work which indicated that chemi-sorption was the main mechanism of selenite removal but inner-sphere complexation did not rule sorption of selenate. High removal capacity to selenate was due to involvement of the interlayer carbonate.

Indeed, in spite of the fact that adsorption of selenite by Mg-Al LDH is higher than of selenate, XRD patterns demonstrated that selenate was present in the interlayer (Fig. S10A) in greater amount than selenite (Fig. S10C).

The presence of selenium aqueous species was reflected by the new peaks (at d=4.24-4.83 Å) indicating formation of the multilayer within the interlayer space of the Mg-Al-CO_3 LDH. These new peaks are due to the presence of selenate and selenite in the interlayer space together with the interlayer carbonate of Mg-Al-CO_3 LDHs, Fig. S10.

We would like to point out that after adsorption of selenate it is not (and it should not be) a Mg-Al-SeO_4 LDHs. It is still Mg-Al-**CO_3** LDH with sorbed (into/within the interlayer) SeO_4^{2-} which replaced gently ***some*** of the ions of CO_3^{2-} and HCO_3^- (both of these carbonate species are present in the interlayer space). This replacement is not to be equivalent exchange of the anions (like one carbonate anion is replaced by one selenate anion).

Similar phenomenon was observed by Kang [7] who discovered formation of the multilayer in the LDH interlayer space due to the presence of the other interlayer species. The authors observed new peaks with d=0.44 and 0.48 nm in the interlayer.

XRD studies showed that selenite was less present in the interlayer space (Fig. S10C) than selenate (Fig. S10A). It is an expected result as inner-sphere complexation was the leading mechanism of its removal as demonstrated by EXAFS studies.

Fig. S10B showing XRD patterns of Mg-Al-CO_3 LDHs with sorbed {selenite+selenate} demonstrates an intermediate results on the presence of the sorbed anions in the interlayer. It is also in correspondence with the adsorption isotherm data (Fig. 1) and EXAFS studies demonstrating that adsorptive capacity to selenite is stronger than to selenate but selenite is less present in the interlayer than selenate.

The interlayer distance (7.74 Å) and the other XRD patterns reflecting the layered structure were not changed after sorption of selenate and selenite. It is an indication that the adsorbent is strong enough what makes it suitable for water treatment. It also means that Mg-Al-**CO_3** LDHs is able to involve its interlayer anions in the removal mechanism (and no need to replace the interlayer carbonate ions for the other anions like Cl-, NO_3^- at al. what is usually done by my researchers).

Increase of the interlayer distances is necessarily happen when the researchers use calcined LDHs using the “memory effect” of LDHs. In this case, the adsorbent is not a layered double

hydroxide with any interlayer anions but a double metal oxide (without layered structure) which, when contacted to water solution, is subjected to rehydration and reconstruction of the original layered structure. During such reconstruction, the available anion(s) are captured into the interlayer space. The interlayer distance will depend on the anion captured into the interlayer space during the reconstruction. For example, Galini [8] studied removal of carmine dye by calcined LDHs; Geng [9] investigated the effect of the synthesis method (direct precipitation or using a urea) on removal of thiosulfate by calcined Mg-Al LDH.

References

[1] W.T.A. Harrison, G.D. Stucky, R.E. Morris, A.K. Cheetam, Synthesis and structure of aluminium selenite trihydrate, $Al_2(SeO_3)_3.3H_2O$, *Acta Cryst.* (1992). C48, 1365-1367.

[2] M.G. Johnston, W.T.A. Harrison, Magnesium selenite dihydrate, $MgSeO_3•2H_2O$. *Acta Cryst*. E57, i24-i25.

[3] S.B. Krivovichev, Crystal chemistry of selenates with mineral-like structures. I. $[Al(H_2O)_6]_2(SeO_4)_3(H_2O)_4$ –the selenate analogue of alunogen. *Proceedings of the Russian Minerological Society*, 2006, 2, 106-113, in Russian.

[4] U. Kolitsch, Magnesium selenate hexahydrate, $MgSeO_4•6H_2O$. *Acta Cryst. Section B*, 2002, 58, i3-i5.

[5] R. Perret, B. Rosso, Parametres de sulphate en selenates trivalent unhydres. Seleniates d'aluminium et de gallium., *Bull. Soc. Chim. Fr.,* 1968, 2700-2701.

[6] G. Jonansson, The crystal structures of $[Al_2(OH)_2(H_2O)_8](SO_4)_2•2H_2O$ and $[Al_2(OH)_2(H_2O)_8](SeO_4)_2•2H_2O$. *Acta Chemica Scandinavica*, 1962, 16, 403-420.

[7] H. Kang, G. Huang, S. Ma, Y. Bai, H. Ma, Y. Li, X. Yang, Coassembly of Inorganic Macromolecule of Exfoliated LDH Nanosheets with Cellulose, *J. Phys. Chem., C* 2009, 113, 9157–9163.

[8] L.El. Galini, M. Lakraimi, E. Sebbar, A. Meghea, M. Bakasse, Removal of indigo carmine dye from water to Mg-Al-CO_3-calcined layered double hydroxides. *J. Haz. Mat.,* 2009, 161, 627-632.

[9] C. Geng, T. Xu, Y. Li, Z. Chang, X. Sun, X. Le, Effect of synthesis method on selective adsorption of thiosulfate by calcined MgAl-layered double hydroxides. *Chem. Eng. J.*, 2013, 232, 510-518.